

ChemComm

Accepted Manuscript



This is an *Accepted Manuscript*, which has been through the Royal Society of Chemistry peer review process and has been accepted for publication.

Accepted Manuscripts are published online shortly after acceptance, before technical editing, formatting and proof reading. Using this free service, authors can make their results available to the community, in citable form, before we publish the edited article. We will replace this *Accepted Manuscript* with the edited and formatted *Advance Article* as soon as it is available.

You can find more information about *Accepted Manuscripts* in the [Information for Authors](#).

Please note that technical editing may introduce minor changes to the text and/or graphics, which may alter content. The journal's standard [Terms & Conditions](#) and the [Ethical guidelines](#) still apply. In no event shall the Royal Society of Chemistry be held responsible for any errors or omissions in this *Accepted Manuscript* or any consequences arising from the use of any information it contains.



www.rsc.org/chemcomm

COMMUNICATION

Atypical Stoichiometry for a 3D Bimetallic Oxalate-Based Long-range Ordered Magnet Exhibiting High Proton Conductivity[‡]

Cite this: DOI: 10.1039/x0xx00000x

Received 00th January 2012,
Accepted 00th January 2012Catalin Maxim,^{a,b,c} Sylvie Ferlay^{a,c,*}, Hiroko Tokoro,^e Shin-Ichi Ohkoshi^e and
Cyrille Train^{b,d,f,*}

DOI: 10.1039/x0xx00000x

www.rsc.org/

The reproducible formation of a 3D oxalate based coordination compound with an unusual Mn^{II}/Cr^{III} ratio, of formula (NH₄)₅[Mn^{II}Cr^{III}₃(ox)₉].10H₂O, is presented. The original topology of the anionic network leads to antiferromagnetic long-range ordering whereas its guests favour high humidity-dependent proton conductivity.

New materials with targeted physical properties are of current interest. Molecular materials are chemically flexible and thus good candidates to reach this goal. Metal-organic frameworks (MOFs)¹ are indeed structurally diverse platforms that allow not only the introduction of a single property such as gas storage, sensors, magnetism or catalysis but also of several properties leading to multifunctional materials. Since their discovery,² oxalate-based extended networks of general formula [M_a^{II/III}M_b^{I/II}(C₂O₄)_n]^{2n-/n-} have focused lot of attention in that direction because the anionic network provide magnetic properties and is able to host a wide variety of functional cations, paving the way to a rational synthesis of magnetic multifunctional materials.³ In particular, electron conduction was observed in such networks through the insertion of tetrathiafulvalene (TTF) cationic stacks between the anionic layers⁴ leading to the synthesis of a molecular ferromagnetic conductor.⁵ A revival of the influence of the electric field recently appears in oxalate-based systems following two distinct objectives: the introduction of ferroelectricity towards molecular multiferroics⁶ and the development of proton conductivity within the material,⁷ a property scarcely observed in MOFs despite its importance for promoting efficient fuel cells.⁸

The strategy develop in the seminal work of Kitagawa *et al.*⁷ on oxalate-based compounds relies on the introduction of acidic or hydrophilic residues into the cationic component in order to construct proton-conductive pathways between the bimetallic layers. Recently, Pardo *et al.*⁹ described an oxalate-based network of formula (NH₄)₄[MnCr₂(ox)₆].4H₂O (**2**) whose proton conduction is related to the presence of ammonium and/or crystallization water molecules within one-dimensional channels. This compound exhibits a three-dimensional (3D) quartz-like coordination network that strongly contrasts with

the well-known 2D (6,3) and 3D (10,3) [M_a^{II/III}M_b^{I/II}(C₂O₄)_n]^{2n-/n-} networks.^{2,3} This example raised questions about (i) the metal stoichiometry and the topology of such networks and (ii) the mechanisms of the proton conduction in such high dimensional architectures.

In this communication, we report the formation of a 3D bimetallic oxalate-bridged compound of formula (NH₄)₅[Mn₂Cr₃(ox)₉].10H₂O (**1**). This 2/3 Mn^{II}/Cr^{III} ratio leads is to an original structure that is described together with the analysis of the magnetic properties and the humidity-dependent conduction properties.

Crystals of **1** were obtained under self-assembly conditions¹⁰ by using a MeOH solution containing ammonium tris(oxalato)chromate(III) and manganese(II) chloride followed by a slow diffusion of a 1/1 CH₃OH/CHCl₃ mixture (see ESI). Whereas the salts are the same than those previously used to obtain bimetallic oxalate-based networks,⁹ it appears that the original solvent mixture used herein addresses reproducibly the unprecedented 2/3 Mn^{II}/Cr^{III} ratio observed in **1**. Originally introduced as a counterion favouring the dissolution of trisoxalatometalate(III) salts in non aqueous solvents, the ammonium cations now appear as template cations of unusual bimetallic oxalate-bridged coordination networks. The observed metal ion ratio corresponds to an original structural arrangement, detailed thereafter, that takes advantage of the robustness of the tris(oxalato)chromate(III) building block and of the versatility of the coordination modes of both the manganese(II) and the oxalate ions.

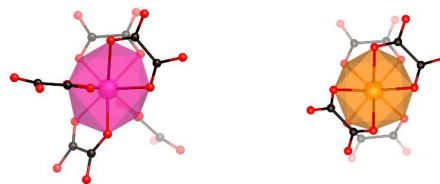


Figure 1: Representation of the Mn coordination environments in **1** for Mn1 (left) and Mn2 (right).

The crystal structure of **1** was solved by single-crystal X-ray diffraction (table S1 in ESI). **1** crystallizes in the achiral C2/c

space group with the formula $(\text{NH}_4)_5[\text{Mn}^{\text{II}}_2\text{Cr}^{\text{III}}_3(\text{ox})_9] \cdot 10\text{H}_2\text{O}$. The dehydration/rehydration process of **1** leads to a partial loss of crystallinity (Fig. S4). The compound is composed of a 3D anionic coordination network with cavities filled by ammonium cations and water molecules. Whereas one of the five ammonium cations needed to balance the charge of the anionic network was solved in the compound, the squeeze command was used for the structural refinement and, on the basis of TGA measurements and elemental analysis, four other ammonium cations and ten water molecules were found to be also present in the network (Fig. S4). Within the network, both independent chromium atoms are surrounded by three oxalate ligands forming a slightly distorted octahedral environment, with Cr-O distances in the 1.963(6) and 2.004(8) Å range. Cr1 is coordinated, via oxalate bridges to three Mn(II) ions in a triangular pyramidal environment, with MnCrMn angles of 102.46, 108.41 and 123.52°, whereas Cr2 behaves as a planar triangular bridge between three Mn atoms in the xOy plane.

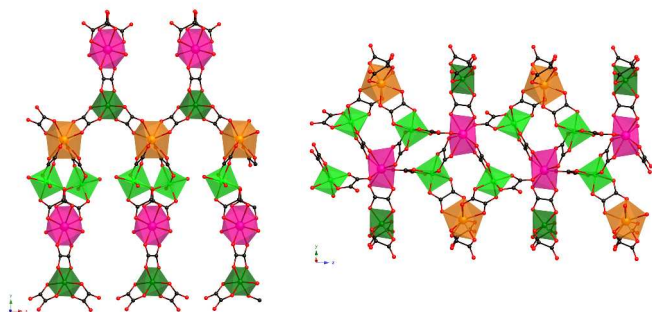


Figure 2: Representation of the bimetallic anionic network in **1** (fuschia= Mn1, gold = Mn2, light green= Cr1, dark green= Cr2) along the *a*-axis (left) and along the *c*-axis (right).

There are two types of manganese(II) in the unit cell. Both are coordinated to eight oxygen atoms located at the vertices of a distorted lozenge antiprism (Fig. 1 and S1). Mn1 is coordinated to two oxygen atoms from different oxalate ligands that act as bidentate-monodentate ligands and to three oxalate ligands in a bis(bidentate) coordination mode (Fig. 1 left and S1 left). The shortest Mn-O distance (2.265(5) Å) corresponds to the monodentate coordination mode. The oxalate ions bridging the two faces of the prism exhibit a short (2.272(4) Å) and a long (2.491(5) Å) Mn-O distances whereas the two oxygen atoms of the bidentate oxalate located on one face of the prism are at 2.342(4) Å of the Mn1 atom. Owing to the mixed coordination modes of the oxalate ligands, Mn1 has coordination links with 5 chromium(III) ions with Mn-Cr distances in the 5.330(6)-5.634(6) Å range (Fig. 2 and S1 left). The situation is simpler for Mn2: it is surrounded by four oxalate ligands in a bis(bidentate) coordination mode (Fig. 1 right and S1 right). Each oxalate occupies an edge of a lozenge and has one short (2.249(5) or 2.267(5) Å) and one long (2.424(6) and 2.367(5) Å respectively) Mn-O distances. It is thus coordinated to four chromium(III) ions being located at distances of Mn2 ranging between 5.574(6) and 5.596(6) Å (Fig. 2 right). To get an overall topological view of the material, one can figure out that both $[\text{Cr}^{\text{III}}(\text{ox})_3]^{3-}$ moieties are connected to 3 Mn(II) ions, whereas the Mn(II) ions act as five and four Cr(III) ions connectors (Fig. 2, left). The topology of the 3D anionic coordination network can be described¹¹ as $\{4.8^4.10\}\{4^2.6\}2\{4^3.6^2.8^3.10^2\}\{8^2.10\}$ point symbol for the four metallic ions representing the network (Mn2, Mn1, Cr2 and Cr1 respectively), which corresponds to 3,3,4,5-*c* network.

This network has never been enumerated in RCSR and Topos.¹¹ The variety of the coordination modes of the oxalate ligand together with the versatility of the octacoordinated manganese(II) ions acting as either four- or five-connectors, allow the formation of this original network.

The anionic network is crossed by two types of channels running along the *a*-axis (Fig. S2 top). The first one is delimited by a distorted lozenge formed by two Cr1 and two Mn1 metal ions. The lozenges are sharing edges along the *c*-axis. The channel section is *ca.* 3.1x4.2 Å². In these channels, one ammonium ion was refined (Fig. S2 bottom). It establishes H-bonds with a terminal oxygen atom of a non-bridging oxalate (O17) with $d_{\text{N-O}}$ distances of 2.940(5) Å and with an oxygen atom of a bridging oxalate ($d_{\text{N-O}} = 2.985(6)$ Å). It is thus in a distorted tetrahedral environment with ONO angles in the range of 55.97 and 144.34°. The second type of channel is delimited by highly flattened octagons. The vertices of each octagon are four Cr1, two Mn1 and two Mn2 metal ions. The channel section is *ca.* 5.4x11.5 Å². Additional electronic density from water molecules and ammonium ions are located in both types of channels, which could not be safely assigned to water molecules or ammonium cations.

The comparison with the 3D parent compounds of formula $(\text{NH}_4)_4[\text{Mn}^{\text{II}}\text{Cr}^{\text{III}}_2(\text{ox})_6] \cdot 4\text{H}_2\text{O}$ (**2**),⁹ and also with $[\text{Ru}(\text{bpy})_2(\text{ppy})][\text{Mn}^{\text{II}}\text{Cr}^{\text{III}}(\text{ox})_3]$ (**3**)^{4c} is important to understand the formation of the coordination network of **1**. In all three compounds **1-3**, the tris(oxalato)chromate(III) tecton is fully preserved. Nevertheless its connections with manganese(II) ions are slightly different. Whereas in **2**, tris(oxalato)chromate(III) acts as a bis(bidentate) metalloligand, in **3**, it acts a tris(bidentate) metalloligand. In **1**, an intermediary situation is reached: as in **3**, Cr2 behaves as a tris(bidentate) metalloligand but Cr1 is a monodentate-bis(bidentate) metalloligand, a situation which is rather scarce.¹² Moreover, **1** differs from other compounds by the environment of the manganese(II) ions. In **1**, Mn2 is surrounded by four bidentate oxalate ligands. This coordination mode appears to be much the same as the one observed in **2**. Nevertheless, the polyhedron evolves from a square antiprism in **1** to a bicapped triangular prism in **2** and, accordingly, the Mn-O distances span over a wider range in the latter compound. Finally, the environment of Mn1 (three bidentate oxalate ligands and two monodentate ones) is the most surprising. In CCDC, it is only found once for a Ba(II) ion in the discrete cluster¹³ but it was never observed for any transition metal ion coordinated by oxalate ions or in any oxalate-based extended coordination network. This unusual coordination environment of Mn1 deeply modifies the connecting rules within the network and leads to the construction of this original coordination network.

The magnetic measurements were performed on microcrystalline powder of **1** checked by PXRD (Fig. S3, ESI). The thermal variations of $\chi_M T$ for **1**, where χ_M is the molar magnetic susceptibility per Mn_2Cr_3 unit and *T* the absolute temperature, is shown in Fig. 3. The $\chi_M T$ value of 14.80 $\text{cm}^3\text{mol}^{-1}\text{K}$ at room temperature is slightly higher than the value calculated for uncoupled magnetic ions ($S_{\text{Mn}} = 5/2$, $S_{\text{Cr}} = 3/2$; $\chi_M T = 14.375 \text{ cm}^3\text{mol}^{-1}\text{K}$ with $g_{\text{Cr}} = g_{\text{Mn}} = 2.0$). $\chi_M T$ increases continuously when *T* decreases, until reaching a maximum value of 35.0 $\text{cm}^3\text{mol}^{-1}\text{K}$ at 6.0 K. The $\chi_M T$ then undergoes an abrupt decrease at low temperature. This behaviour is indicative of dominant Mn-Cr ferromagnetic (F) exchange interaction through the oxalate bridge. To quantify this interaction, the thermal variation of the inverse of the susceptibility was fitted by a Curie-Weiss law between 20 and 300 K leading to a value

of the Curie-Weiss temperature $\Theta = 4.0$ K (Fig. 3 left). Moreover, the field-cooled magnetization (FCM) exhibits a peak at $T_N = 6.0$ K which is indicative of the onset of an antiferromagnetic (AF) order (Fig. 3, right).

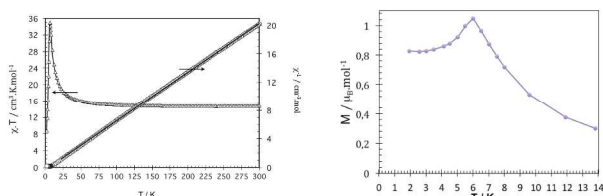


Figure 3: Thermal dependence of $\chi_M T$ and χ_M^{-1} (left) and field-cooled magnetization (FCM) for **1** (right).

There seems to be a contradiction between the nature of the exchange interaction deduced from the treatment of the susceptibility and the nature of the long-range magnetic order (LRMO) deduced from the FCM. The comparison between the Curie-Weiss and the Néel temperatures is the first element to solve this ambiguity. The Curie-Weiss temperature can be related to the exchange interaction parameters using a mean-field approach known as molecular field.¹⁴ This has two consequences: (i) when only one interaction is present the absolute value of the Curie-Weiss temperature is always *greater* than the LRMO temperature (ii) when several exchange interaction are present, the Curie-Weiss temperature averages the different exchange interaction parameters. In the case of **1**, it means that a dominant F interaction coexists with either a weaker F interaction or even an AF one. The latter situation is the only compatible with the onset of an AF LRMO. A close look at the structure brings complementary information on the nature of the exchange interaction. In the [MnCr] oxalate-bridged networks, the Mn-Cr exchange interaction is F when the oxalate bridge is symmetric. On the contrary, it becomes AF when the bridge is fairly unsymmetrical with respect to the manganese(II) ion as found in $[\text{Mn}(\text{CH}_3\text{OH})_6][\text{Mn}(\text{CH}_3\text{OH})\text{Cr}(\text{ox})_3]_2 \cdot 2\text{CH}_3\text{OH}$.¹⁵ Though the structure of **1** is rather complicated, these guidelines can be followed for a first magneto-structural analysis. In the (*ab*) planes (Fig. 2 left), all the oxalate ligands are in a rather symmetrical bis(bidentate) bridging mode. Accordingly, the exchange interaction in these planes is F. In the (*bc*) planes (Fig. 2 right), the situation is more complicated. Along the *b*-axis, the interaction is F. But along the *c*-axis, the oxalate ligands bridging Mn1 to Cr1 adopt a bidentate-monodentate mode which is the extreme case of the dissymmetrical bridge observed in ref. 15. Accordingly, the interaction along this direction is AF. The contribution of this latter interaction to the Curie-Weiss temperature leads to a decrease of its value. Moreover, it couples AF the F-coupled (*ab*) planes leading to an overall AF LRMO.

Electrical measurements were performed on sintered microcrystalline powder of **1** at 298 K at various humidity rates (Fig. 4 and S5 in ESI). For example, for a relative humidity (RH) set at 74% of the saturation value, a Cole-Cole circular arc fitting of the curve leads to a conductivity value σ of $7.1 \cdot 10^4$ S cm^{-1} (Fig. 4 left).¹⁶ Let us note that the value of 74%RH is the maximum we can reach in the case of **1** because above 80%RH, the crystals are deliquescent, preventing measuring their conducting properties. When the relative humidity is decreased, the σ values undergo a dramatic decrease of five orders of magnitude down to $9.1 \cdot 10^{-9}$ S cm^{-1} at 9.5 %RH (Fig. 4, right). This behaviour is much similar to what has been observed in other oxalate-based anionic networks hosting acidic

cation.^{7,9} The strong dependence of the conductivity upon relative humidity confirms that proton conductivity is responsible for the high conductivity of **1** and should occur through a Grotthuss mechanism.¹⁷

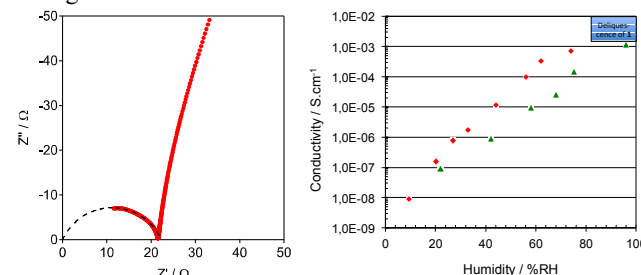


Figure 4: Cole-Cole plot for the conductivity of **1** measured in 74 %RH at 298 K (left) and dependence of the conductivity of **1** (red losange) and **2** (green triangle) at 298 K with the relative humidity around the sample (for **2**, the data are extracted from ref. 9) (right).

Compared to the parent 3D compound **2**,⁹ the conductivity of **1** is slightly higher at comparable RH (Fig. 4 right). In the present case, a possible explanation for the increase of the protonic conductivity could be based on the enlargement of the channels section in **1** compared to the one in **2**, in particular for the octagonal ones. In turn, this enhanced accessibility to water molecules could also explained the deliquescent behaviour of compound **1** at high RH percentages. Nevertheless, in contrast with the most fruitful magnetostructural approach, the main difficulty to correlate the structure of proton conductors to their electrical behaviour, is that the identification and localisation of the molecules responsible for the conduction by X-ray diffraction are next to impossible.

Conclusions

The synthesis of a bimetallic oxalate-bridged system, in $\text{CH}_3\text{OH}/\text{CHCl}_3$ diffusion mixture yields a three dimensional compound of formula $(\text{NH}_4)_5[\text{Mn}_2\text{Cr}_3(\text{ox})_9] \cdot 10\text{H}_2\text{O}$ presenting a remarkable $\text{Mn}^{\text{II}}/\text{Cr}^{\text{III}}$ ratio. In this compound, the coordination of the manganese(II) ions are original and, by modifying the connection rules of this ion, leads to an intriguing three-dimensional 3,3,4,5-c network. Moreover, the architecture displays wide channels filled with water and ammonium molecules. These guests are responsible for a high proton conductivity of the compound. In addition, this proton conductor displays a long-range magnetic ordering with $T_N = 6\text{K}$.

Acknowledgement

Pr. M. W. Hosseini and Pr. Marc Henry are acknowledged for fruitful discussions and help in Topos use. This work was supported by the Centre National de la Recherche Scientifique (CNRS), Université de Strasbourg (UdS), Université Joseph Fourier (UJF), Institut Universitaire de France (IUF) and the Agence Nationale de la Recherche (ANR) within the framework of the ANR-08-JCJC-0113-01 project in particular through a postdoctoral grant to C. M.

Notes and references

^a Molecular Tectonic Laboratory, UMR UDS-CNRS 7140, Université de Strasbourg, Institut Le Bel, 4, rue Blaise Pascal, F-67000 Strasbourg, France

^b CNRS, LNCMI, 25 rue des Martyrs, B.P. 166, F-38042 Grenoble cedex 9, France

^c University of Bucharest, Faculty of Chemistry, Inorganic Chemistry Laboratory, Str. Dumbrava Rosie nr. 23, 020464-Bucharest, Romania.

^d Institut Universitaire de France (IUF)

^e Department of Chemistry, School of Science, University of Tokyo, Tokyo 113-0033, Japan.

^f Univ. Grenoble Alpes, LNCMI, F-38041 Grenoble Cedex 9, France

E-mail : cyrille.train@lncmi.cnrs.fr, ferlay@unistra.fr

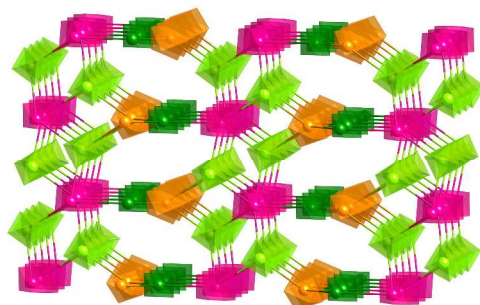
† Electronic Supplementary Information (ESI) available: Complete experimental part, X ray diffraction data (CCDC 981441), XRPD patterns, TGA traces and conductivity properties. See DOI: 10.1039/c000000x/

‡ Dedicated to Academician Pr. Andruh (University of Bucharest) at the occasion of his 60th birthday

- [1] (a) S. R. Batten and R. Robson, *Angew. Chem., Int. Ed.*, 1998, **37**, 1460-1494; (b) C. Janiak and J. K. Vieth, *New J. Chem.*, 2010, **34**, 2366-2388; (c) *Chem. Rev.*, 2012, **112**, themed issue on metal-organic frameworks.
- [2] M. Ohba, H. Tamaki, N. Matsumoto and H. Okawa, *Inorg. Chem.*, 1993, **32**, 5385-5390.
- [3] (a) S. Decurtins, H. W. Schmalte, P. Schneuwly, J. Enslin and P. Gütllich, *J. Am. Chem. Soc.* 1994, **116**, 9521-9528; (b) M. Hernández-Molina, F. Lloret, C. Ruiz-Pérez, M. Julve, *Inorg. Chem.* 1998, **37**, 4131-4135; (c) M. Gruselle, R. Andrés, B. Malézieux, M. Brissard, C. Train, M. Verdaguer, *Chirality*, 2001, **13**, 712-714; (d) M. Clemente-León, E. Coronado, C. J. Gómez-García and A. Soriano-Portillo, *Inorg. Chem.*, 2006, **45**, 5653-5660; (e) F. Pointillart, C. Train, F. Villain, C. Cartier dit Moulin, P. Gredin, L.-M. Chamoreau, M. Gruselle, G. Aullon, S. Alvarez, M. Verdaguer, *J. Am. Chem. Soc.*, 2007, **129**, 1327-1334.
- [4] M. Kurmoo, A.W. Graham, P. Day, S. J Coles, M. B. Hursthouse, J. L. Caulfield, J. Singleton, F. L. Pratt, W. Hayes, L. Ducasse, P. Guionneau, *J. Am. Chem. Soc.* 1995, **117**, 12209-12217.
- [5] E. Coronado, J. R. Galán-Mascarós, C. J. Gómez-García V. Laukhin, *Nature* 2000, **408**, 447-449.
- [6] E. Pardo, C. Train, H. Liu, L.-M. Chamoreau, B. Dhkil, K. Boubekeur, F. Lloret, K. Nakatani, H. Tokoro, S. Ohkoshi, M. Verdaguer *Angew. Chem., Int. Ed.*, 2012, **51**, 8356-8360.
- [7] (a) H. Ōkawa, A. Shigematsu, M. Sadakiyo, T. Miyagawa, K. Yoneda, M. Ohba and H. Kitagawa *J. Am. Chem. Soc.* 2009, **131**, 13516-13522; (b) M. Sadakiyo, H. Ōkawa, A. Shigematsu, M. Ohba, T. Yamada and H. Kitagawa *J. Am. Chem. Soc.* 2012, **134**, 5472-5475; (c) H. Ōkawa, M. Sadakiyo, T. Yamada, M. Maesato, M. Ohba and H. Kitagawa *J. Am. Chem. Soc.* 2013, **135**, 2256-2262; (d) T. Yamada, K. Otsubo, R. Makiurac and H. Kitagawa *Chem. Soc. Rev.*, 2013, **42**, 6655-6669.
- [8] (a) G. Ferey, F. Millange, M. Morcrette, C. Serre, M. L. Doublet, J. M. Greneche and J.-M. Tarascon, *Angew. Chem. Int. Ed.*, 2007, **46**, 3259-3263; (b) S. Bureekaew, S. Horike, M. Higuchi, M. Mizuno, T. Kawamura, D. Tanaka, N. Yanai and S. Kitagawa *Nat. Mater.* 2009, **8**, 831-836; (c) J.A. Hurd, R. Vaidhyanathan, V. Thangadurai, C.I. Ratcliffe, I.L. Moudrakovski and G.K.H. Shimizu *Nat. Chem.* 2009, **1**, 705-710; (d) S. Ohkoshi, K. Nakagawa, K. Tomono, K. Imoto, Y. Tsunobuchi and H. Tokoro *J. Am. Chem. Soc.* 2010, **132**, 6620-6621; (e) N. C. Jeong, B. Samanta, C. Y. Lee, O. K. Farha, and J. T. Hupp *J. Am. Chem. Soc.*, 2012, **134**, 51-54.
- [9] E. Pardo, C. Train, G. Gontard, K. Boubekeur, O. Fabelo, H. Liu, B. Dhkil, F. Lloret, K. Nakagawa, H. Tokoro, S.-I. Ohkoshi and M. Verdaguer *J. Am. Chem. Soc.*, 2010, **133**, 15328-15331.
- [10] S. Mann, *Nature*, 1993, **365**, 499-505.
- [11] (a) V. A. Blatov, TOPOS, a Multipurpose Crystallochemical Analysis with the Program Package; Samara State University: Russia, 2004. (b) Reticular Chemistry Structure Resource (RCSR), the associated website, <http://okeeffe-ws1.la.asu.edu/RCSR/home.htm>.
- [12] (a) G. Ballester, E. Coronado, C. Gimenez-Saiz, F. M. Romero, *Angew. Chem. Int. Ed.* 2001, **40**, 792-795; (b) H.-Z. Kou, O. Sato, *Inorg. Chem.*, 2007, **46**, 9513-9515; (c) E. Coronado, J. R. Galán-Mascaros, C. Martí-Gastaldo, *Inorg. Chim. Acta*, 2008, **361**, 4017-4023.
- [13] B.-L. Fei, R. Clerac, C. E. Anson, A. K. Powell, *Dalton Trans.*, 2005, 1381-1386.
- [14] (a) A. Herpin, Théorie du magnétisme, Bibliothèque des sciences et techniques nucléaires, 1968; (b) S. Ohkoshi, K. Hashimoto, *J. Am. Chem. Soc.*, 1999, **121**, 10591-10597.
- [15] E. Coronado, J. R. Galán-Mascaros, C. Martí-Gastaldo, A. M. Martínez, *Dalton Trans.*, 2006, 3294-3299.
- [16] The other experiments done by varying the relative humidity (RH) are given in ESI.
- [17] P. Colomban, Proton Conductors: Solids, Membranes and Gels-Materials and Devices, Cambridge University Press, Cambridge, U.K., 1992.

COMMUNICATION

Graphical abstract



A 3D achiral oxalate based coordination compound of formula $(\text{NH}_4)_5[\text{Mn}^{\text{II}}_2\text{Cr}^{\text{III}}_3(\text{ox})_9]\cdot 10\text{H}_2\text{O}$, with an unusual $\text{Mn}^{\text{II}}/\text{Cr}^{\text{III}}$ ratio exhibits an antiferromagnetic long-range ordering whereas its guests favour high proton conductivity.